Sensors & Transducers, Vol. 171, Issue 5, May 2014, pp. 176-182

Sensors & Transducers

Application of Optical Measurement Method in Brazilian Disk Splitting Experiment Under Dynamic Loading

[1, 2] Zhiqiang YIN, [1, 2] Lei WANG, [3] Haifeng MA, [1, 2] Zuxiang HU and [4] Jiefang JIN

[1] The Provincial Key Laboratory of Mining Effects and Disasters Preventing under Deep Mining in Anhui, Anhui University of Science and Technology, Huainan 232001, China
[2] School of Mineral and Safety, Anhui University of Science and Technology, Huainan 232001, China
[3] Faculty of Resources and Safety Engineering, China University of Mining and Technology, Beijing 100083, China
[4] School of Architectural and Surveying Engineering, Jiangxi University of Science and Technology, Ganzhou 341000, China
[1] Tel.: 0554-6633285, fax: 0554-6633285
E-mail: zhqyin@aust.edu.cn

Received: 23 April 2014 /Accepted: 27 May 2014 /Published: 31 May 2014

Abstract: A real-time and in situ optical measuring system is developed, which can be used to observe the determination of the displaced field on Brazilian disk splitting under dynamic loading. The system consists of high speed (HS) photography, split-Hopkinson pressure bar (SHPB), synchronization controlling system and the operation of differential image. In the present experiments, photographs of the specimen were taken using a FASTCAM SA1.1 high speed camera, the frame rate was 100,000 fps. The continuous images of rock sample dynamic Brazil fracturing process and stress wave loading on the specimen were observed by synchronization controlling system. The change law of surface displacement field was calculated from the method of differential image base on the joint probability distribution function of two images. This method was considered the image correlation, and effectively eliminated the influence of background noise, and could identify the surface displacement and the occurrence and expansion of the crack in the dynamic Brazilian disk splitting experiments straightforward and effectively. This method can provide a novel measurement of surface displacement field in Brazilian disk splitting tests under high strain rates. *Copyright © 2014 IFSA Publishing, S. L.*

Keywords: SHPB, Brazilian disk, Dynamic loading, High-speed photography, Differential image.

1. Introduction

The tensile characteristic is an important characteristic of rock. Rocks are much weaker in tension than in compression. So, the big reason of failure of rock structure is from tensile stress. It is thus important to characterize the tensile strength of rocks in general and to understand the correlation between strength and the microcrack-induced in particular [1]. In many rock engineering, such as mining and civil engineering, in the circumstances of rock excavation the surrounding rock is not only under static stress, but also under dynamic stress, such as, rock cutting, tunneling, drilling, blasting, rock bursts and other dynamic loads. The researchers found statistically significant difference in mechanics

performance of rock between dynamic loads and static loads [2]. Along with the deepening of research, as researchers more fiercely study on transient response of rock failure under dynamic loads, and accurate description of deformation and fracture characteristics in particular.

Among dynamic loading apparatus, the split-Hopkinson pressure bar (SHPB) is widely used. The SHPB is a standard apparatus for measuring the mechanical properties of materials at strain rates between 101 and 104 s-1. As early as 1968s, SHPB tests were conducted on basalt and granite to investigate the strain rate and temperature effect [3]. In recent years, the method has been further taken experimentally to investigate dynamic tensile strength and dynamic characteristics subjected to intermediate loading rate of rocks [4-6]. This experiment method to measure mechanical property was based on the one-dimensional elastic wave theory, which elastic wave was measured from the signals of strain gauges on the input and output bars. Since the strain-to-failure of brittle materials is very small, indirectly obtained strains from the signals of strain gauges on the bars are not very accurate, and thus non-contact full-field measurement techniques should be introduced to provide reliable results.

The digital image method is widely used in experimental mechanics as a practical and effective tool for full-field deformation measurement [7]. In static or slow events, standard cameras provide very good quality data, based on such a wealth of experimental digital image data, some new test procedures to calculate the surface displacement and deformation have been development [8]. In dynamic event (impact, Hopkinson bar tests), because of the small displacements involved, these experiments require the ability of displacement metrology to produce measurements of a higher resolution than the camera used. So, for dynamic events, this area of research is still very much in its infancy. The high speed camera and digital image method have the fast development in recent years. The deformation and crack characteristic of rock under dynamic loading have been studied by many researchers. Siviour [9] used a high speed camera for the high strain rate experiment, in which specimen deformation was monitored and fields' method of a three point bending was analyzed.

In this work, we use a 50 mm SHPB system to load the Brazilian disc specimen, and a high speed camera was used to monitor the full-field deferment fracture process of the specimen. Based on the method of differential image base on the joint probability distribution function of two images, the surface deformation and failure mode of specimen were analyzed.

2. Digital Image Processing Method

The small distortion of specimen is not easy to be recognized especially for dynamic loading. Very tiny changes can be detected by image difference method, which analyses the pixels at the same corresponding position in the two images. The image subtraction techniques described here are based on the use of a scatter gram of a sample of image data as a basis for a statistical model.

This method devised for calculating the difference image used the probability distributions in the normalized scatter gram directly. It defined a probability that reflected how likely it was that the grey level values from corresponding pixels in an image pair were drawn from the same distribution as the rest of the data. Corresponding pairs of pixels from the original images were taken, and their grey levels used to find their coordinates in the normalized scattergram [10]. Integration was then performed along the vertical cut passing through that point c, summing all of the values $F(x, y)$ smaller than the value $F(x, c)$ at that point.

$$D(x,y)=\sum_{c}\delta(F(x,c)>F(x,y))F(x,c), \quad (1)$$

The image of $g_1(x, y)$ and $g_2(x, y)$ are the grey values of the subset in the non-deformed and deformed images, respectively. The m and n are the probability distribution density of the grey values of images respectively. The $S(m, n)$ is probability distribution of the pixel gray distribution with g_1 and g_2 . The image difference S can reflect the probability of grey values different between two images at same regional. So, when the image of $g_1(x, y)$ and $g_2(x, y)$ were completely identical, S=0. When the background noise of images was no change, S was direct finite difference, such as:

$$S=abs[g_1(x,y)-g_2(x,y)], \quad (2)$$

When the background noise of images was change, S was equal to stack values of weighted average background noise and grey. By this means eliminating effect of background noise.

3. Experimental Setup

3.1. Sample Preparation

The rock material used in the study was fine-grained sandstone available in the Zigong of Sichuan, China. In the present study BD tests were performed for measuring surface deformation. The BD tests specimen was made with the dimensions of 50 (diameter)×20 (length) mm. The non-parallelism and the non-perpendicularity of specimen are both less than 0.02 mm. The specimen is gray and smooth on surface, with no distinct interspace. The density of specimen is 2.50 t/m^3.

3.2. Experimental Setup

A schematic of experimental setup is shown in Fig. 1. The stress transmission component is made up

of two long elastic bars (input bar, output bar). The elastic bars are 2 m in length and 50 mm in diameter. The specimen is sandwiched between the two elastic bars [11]. A conical bullet is used in the improved test system to eliminate the oscillation, and obtain a stable half sine wave loading [12-14]. Strain gauges are glued on the surface of the middle of elastic bars to measure strain histories induced by the stress waves propagating along the elastic bars. The material quality of the bullet and the maximum diameter of the projectile body are the same as those of the input bar and output bar. The stress waves recorded with a CS-1D super dynamic meter and DL 750 oscilloscope (Yokogawa). The striking velocity was measured by a laser-beam velocity measurement system.

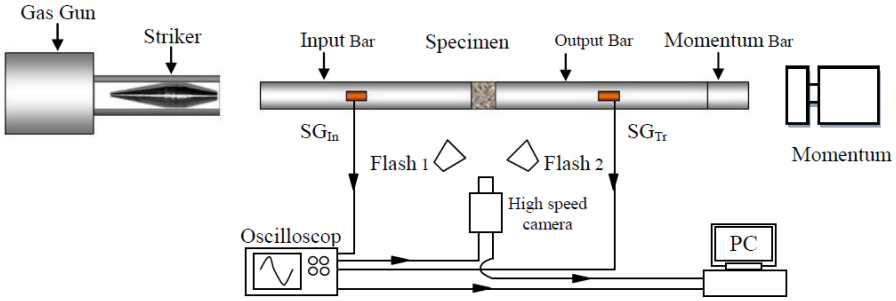

Fig. 1. Schematic of the split Hopkinson pressure bar system.

3.3. Data Acquisition and Processing

i) Data acquisition of SHPB.

Favorable locations for the strain gauges are ideally such that the incident and reflected waves do not overlap as shown in Fig. 2 [15]. In the present study, BHF strain gauges manufactured by Huang-yan Instruments Co., China, with measuring grid size 2×1mm^2 (length×width) were used for the strain measurement. Strain gauges require a DC power supply and a Wheatstone bridge for signal amplification. Strains are extracted from measured signals using bridge amplification and the calibrated gauge factor. A detailed valuation of the effect of the position and orientation of strain gauges on the determination of experimental results is critically presented.

And then strain gauge signals are recorded using a HS-digital oscilloscope with a higher sampling rate (10 MS/s) and a 12-bit isolation module and preferably with differential inputs to reduce noise. The threshold of electric potential of Transistor–Transistor-Logic (TTL) pulse generated by strain gauge on the incident bar should be preset to trigger the oscilloscope. All of the raw data just as observed on the oscilloscope are processed as described after being digitally filtered with a low-pass filter with a cutoff frequency of 10,000 Hz.

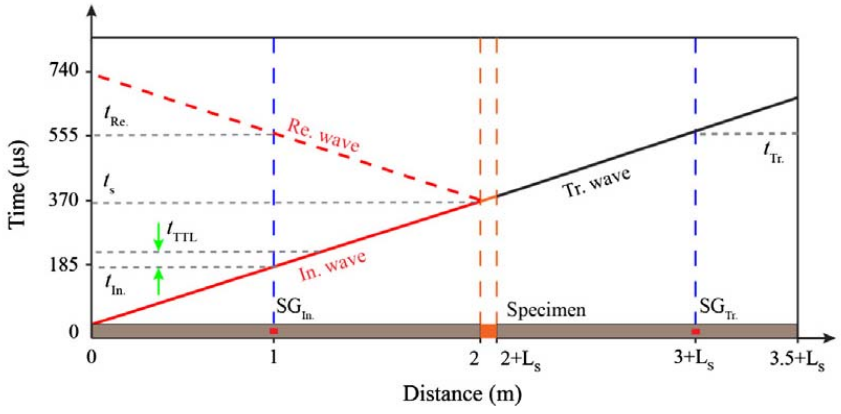

Fig. 2. Lagrangian wave propagation diagram.

This is done to remove the very high frequency bit noise that over lays the strain signals and resulted in robust algorithms for detecting the time-of-arrival of the stress wave.

ii) 3-wave analysis.

The ramped wave produced by the cone-shaped striker lengthens the rise time of the incident stress wave allowing the specimen to equilibrate during the

time of interest for the test. Since the strains in the elastic bars are known, a procedure calculates the normal forces at the two bar/ specimen interfaces as

$$P_1 = E_b A_b (\varepsilon_I + \varepsilon_R), \quad P_2 = E_b A_b \varepsilon_T \tag{3}$$

where E_b is the Young's modulus of the bar, A_b is the cross-sectional area of the bar, and ε_I, ε_R and ε_T are the incident, reflected and transmitted strains measured by strain gauges on the bars.

The typical approach to check stress equilibrium involves a comparison of the force histories at the two sides of the specimen. If the forces are nearly equal, then the specimen is said to be in stress equilibrium. The mean force applied on the specimen can be derived as,

$$P(t) = \frac{1}{2}(P_1 + P_2) - \frac{1}{2} E_b A_b (\varepsilon_I + \varepsilon_R + \varepsilon_T), \tag{4}$$

Under the condition of stress equilibrium, the dynamic tensile strength (σ_{td}) can be derived by using the applied dynamic load ($P(t)$) and the time-to-fracture (t_f):

$$\sigma_{td}(\dot{\sigma}_{td}) = \frac{2P(t_f)}{\pi DB}, \tag{5}$$

where D is the specimen diameter, B is the specimen thickness.

The loading rate ($\dot{\sigma}_{td}$) is determined by the slope of the stress history starting from the time of stress equilibrium (t_{equil}) and ending to the time-to-fracture (t_f).

iii) High speed camera system

In the present experiment, photographs of the specimen were taken using a PHOTRON FASTCAM SA1.1 high speed camera, coupled with a PALLITE high strength and no stroboscopic light source and positioned at 0.7 m away from the specimen surface. The frame-rate of 100,000 fps with an image resolution of 192 pixels×192 pixels and a shutter speed of 1 μs was selected. The specimen was speckled with black and white paint. The photographic view of dynamic testing methods was shown in Fig. 3.

A triggering system is composed of strain gauges (which one is on the surface of the input bar) and oscilloscope. When the bullet hits the input bar, the stress wave is produced and propagating in the input bar. A TTL electrical signal which can be used for triggering will be generated when the oscilloscope recording this stress wave signal by strain gauges. The high speed camera was triggered by a TTL pulse and synchronized with in 100 ns time delay using 2 m network cable connecting to an oscilloscope. Therefore the time of capturing HS-images started from the time triggered by the TTL pulse, and the number of captured images could be obtained until the stress wave arrived at the specimen,

$$n = \frac{t_s - t_{In} - t_{TTL}}{t_{frame}}, \tag{6}$$

where t_s is the time-of-arrival of the specimen, t_{In} is the time-of-arrival of the incident wave, t_{TTL} is the time triggered by a TTL pulse that is determined from the incident wave data, as clearly indicated and shown in Fig. 2, and t_{frame} is the inter-frame time of HS-camera.

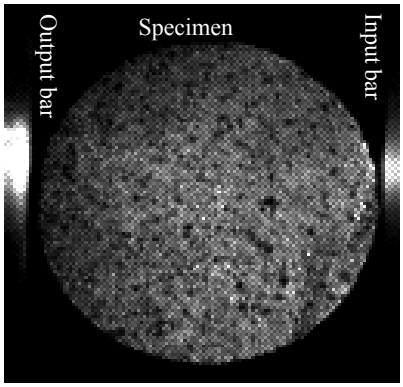

Fig. 3. Photographic view of dynamic testing.

In this test, to match the recorded images with the loading steps, delay time from the loading start time to the triggering start time has been to determine to be 188 μs, based on the combined consideration of the travel time from strain gauge to the specimen end (wave velocity 5410 m/s, distance 1017 mm) and the pre trigger time by a TTL pulse 26 μs which is show in Fig. 4.

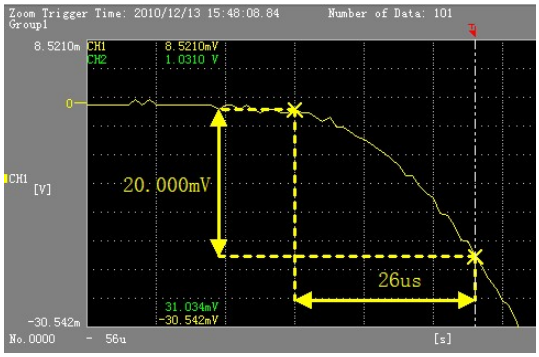

Fig. 4. The pre trigger time measurement.

4. Results and Discussion

Fig. 5 represented a typical testing result with a striking velocity of 3 m/s. It can be seen from Fig. 5(b) that the time of stress equilibrium was

approximately 48 μs, and the time-to-fracture was about 80 μs, according to the corresponding time of the peak load. Fig. 6 shows tensile stress time history with high speed images, the dynamic tensile strength was about 14.2 MPa at the loading rate 202 GPa/s, as shown in Fig. 6. The first image (2 μs) was chosen as the reference image, as shown in Fig. 7. The differential images are shown in Fig. 8.

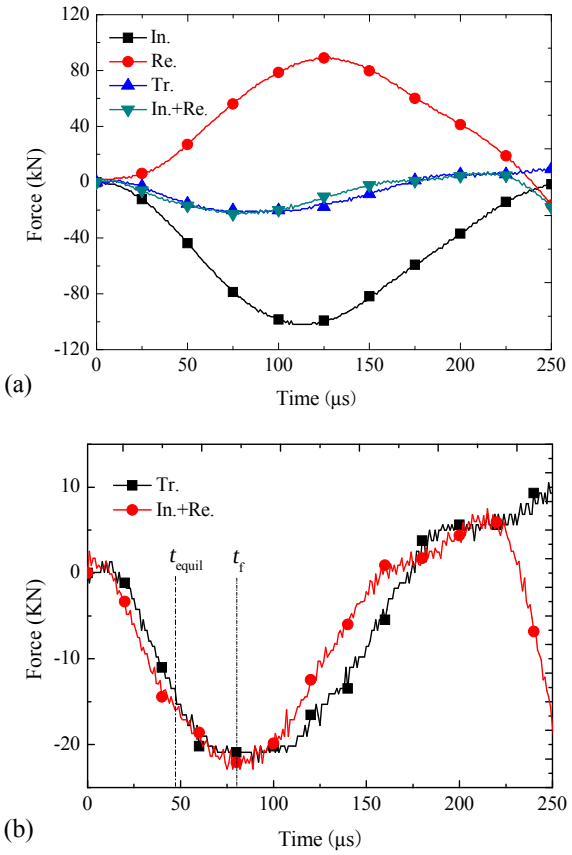

Fig. 5. Dynamic force balance check for dynamic Brazilian experiment.

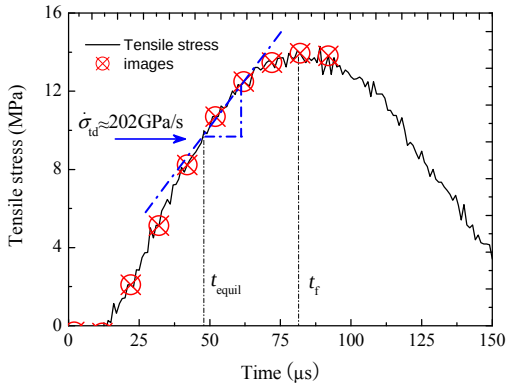

Fig. 6. Stress-time history with high speed images.

The results of image difference technique reproduced the main deformation process and validate the accurate of BD test under dynamic loads. The white spots in Fig. 8 are said the deformation of the surface of rock specimen.

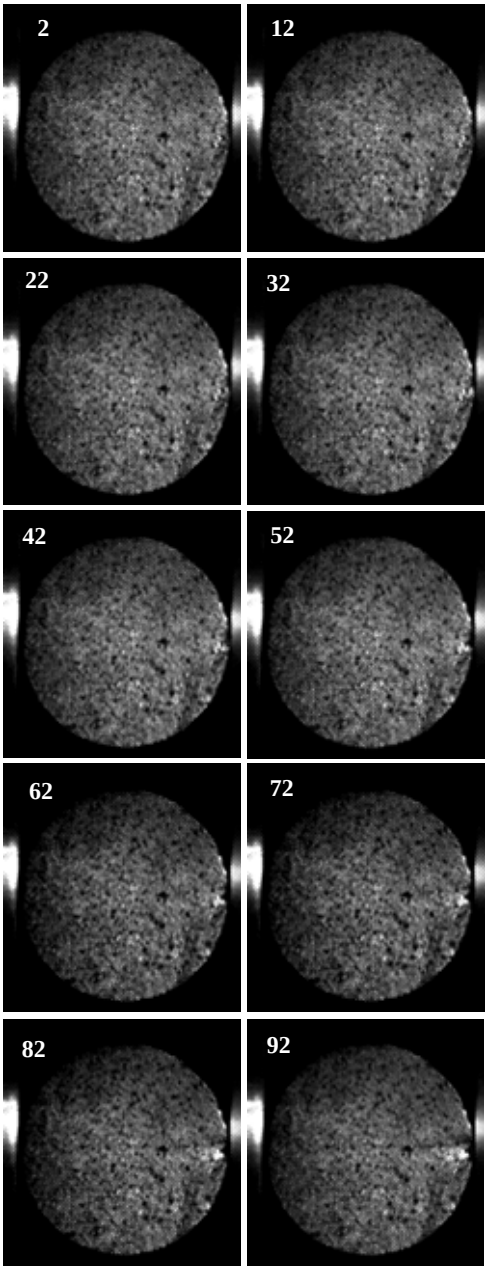

Fig. 7. High speed images.

A the time of before 48 μs, which the time of stress equilibrium between input bar and output bar, those spots of white emerged from the right end of specimen and began spreading to left end and getting larger. This result is consistent with a dynamic photoelastic numerical simulation on the heterogeneous specimen [16]. Between the time of stress equilibrium (48 μs) and the time-to-fracture (80 μs), the spots of white and the tensile stress (Fig. 6) both increased gradually. Then after the time-to-fracture (80 μs), observable crack (block line in Fig. 8 (82 μs, 92 μs)) initiated at the center of disc along the loading line, and the tensile stress decreases

with time (Fig. 6). The failure pattern at time 80 μs closely resembles to the experimental results of fine-grained marble obtained by Q.B. Zhang [16].

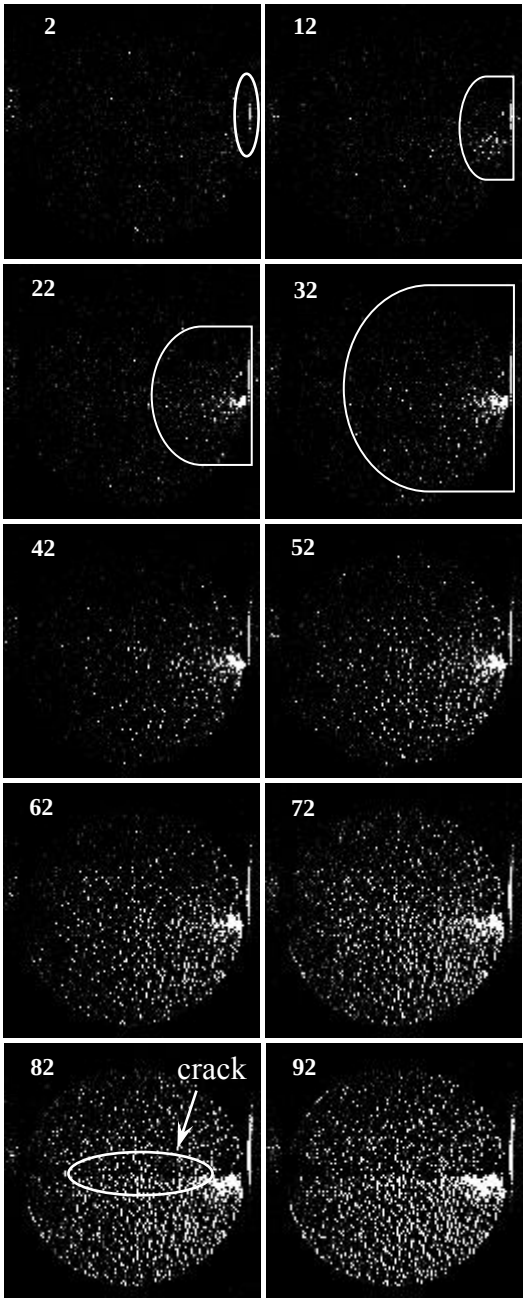

Fig. 8. Differential images.

5. Conclusions

In this work, the method combining a dynamic loading with the differential image technique was successfully used to study the dynamic fracture behavior of sandstone. Based on laboratory investigations and obtained results in this study, the following conclusions can be drawn:

1) In this work, the method combining a SHPB with the HS camera technique was successfully used to study the dynamic fracture behavior of sandstone. In situ images of the surface of sandstone in Brazilian disk test were acquired during dynamic loading step.

2) The image difference technology base on probability integration in conjunction with HS- photography was used to measure full-field deformation of specimens. The proposed system allows the cost-effective, non- contact full-field deformation measurements of specimens in dynamic testing methods. It is found from the experimental results that the dynamic mechanical properties can be well determined and the image difference technology base on probability integration is a reliable full-field deformation measurement method.

3) It is expected to become increasingly popular in the future as increasingly higher speed and higher resolution cameras and increased computing methods, especially in subpixel techniques become more readily and economically available.

Acknowledgements

This work was financially supported by the National Natural Science Foundation of China (No. 51304007, 51104004, 51104068), the State Key Program of National Natural Science Foundation of China (U1361208), China Postdoctoral Science Foundation (No. 2013M531495) and Scientific Research Fund for Young Teachers of Anhui University of Science and Technology (No. 2012QNY39).

References

[1]. F. Dai, K. W. Xia, L. Tang, Rate dependence of the flexural tensile strength of Laurentian granite, *International Journal of Rock Mechanics and Mining Science*, Vol. 47, Issue 3, 2010, pp. 469-475.

[2]. Z. X. Zhang, S. Q. Kou, J. Yu, et al, Effects of loading rate on rock fracture, *International Journal of Rock Mechanics and Mining Sciences*, Vol. 36, Issue 5, 1999, pp. 597-611.

[3]. A. Kumar, The effect of stress rate and temperature on the strength of basalt and granite, *Geophysics*, Vol. 33, Issue 3, 1968, pp. 501-510.

[4]. Q. Z. Wang, F. Feng, M. Ni, et al, Measurement of mode I and mode II rock dynamic fracture toughness with cracked straight through flattened Brazilian disc impacted by split Hopkinson pressure bar, *Engineering Fracture Mechanics*, Vol. 78, Issue 12, 2011, pp. 2455-2469.

[5]. J. F. Jin, X. B. Li, H. B. Zhong, Study of dynamic mechanical characteristic of sandstone subjected to three-dimensional coupled static-cyclic impact loadings, *Chinese Journal of Rock Mechanics and Engineering*, Vol. 32, Issue 7, 2013, pp. 1358-1372.

[6]. X. B. Li, T. S. Lok, J. Zhao, Dynamic characteristics of granite subjected to intermediate loading rate, *Rock Mechanics and Rock Engineering*, Vol. 38, Issue 1, 2005, pp. 21-39.

[7]. W. H. Peters, W. F. Ranson, Digital imaging techniques in experimental stress analysis, *Optical Engineering*, Vol. 21, Issue 3, 1982, pp. 427-431.

[8]. Y. I. Song, S. P. Ma, X. B. Yang, et al, Experimental investigation on failure of rock by digital speckle correlation methods, *Chinese Journal of Rock Mechanics and Engineering*, Vol. 30, Issue 1, 2011, pp. 170-175.
[9]. C. R. Siviour, S. G. Grantham, D. M. Williamson, et al, Novel measurements of material properties at high rates of strain using speckle metrology, *The Imaging Science Journal*, Vol. 57, Issue 6, 2009, pp. 326-332.
[10]. Z. Q. Yin, X. B. Li, T. B. Yin, et al, Critical failure characteristics of high stress rock inducer by impact disturbance under confining pressure unloading, *Chinese Journal of Rock Mechanics and Engineering*, Vol. 31, Issue 7, 2012, pp. 1355-1362.
[11]. X. B. Li, T. S. Lok, J. Zhao, et al, Oscillation elimination in the Hopkinson bar apparatus to complete dynamic stress-strain curves for rocks, *International Journal of Rock Mechanics and Mining Science*, Vol. 37, Issue 7, 2000, pp. 1055-1060.
[12]. X. B. Li, D. S. Gu, H. H. Lai, On the reasonable loading stress waveforms determined by dynamic stress-strain curves of rock by SHPB, *Explosion and Shock Waves*, Vol. 13, Issue 2, 1993, pp. 125-130.
[13]. Z. L. Zhou, X. B. Li, X. M. Yan, Loading condition for specimen deformation at constant strain rate in SHPB test of rocks, *Chinese Journal of Rock Mechanics and Engineering*, Vol. 28, Issue 12, 2009, pp. 2445-2452.
[14]. Q. B. Zhang, J. Zhao, Determination of mechanical properties and full-field strain measurements of rock material under dynamic loads, *International Journal of Rock Mechanics and Mining Sciences*, Vol. 60, Issue 6, 2013, pp. 423-439.
[15]. S. K. Khanna, A. Shukla, On the use of strain gages in dynamic fracture mechanics, *Engineering Fracture Mechanics*, Vol. 51, Issue 6, 1995, pp. 933–948.
[16]. W. C. Zhu, C. A. Tang, Numerical simulation of Brazilian disk rock failure under static and dynamic loading, *International Journal of Rock Mechanics and Mining Sciences*, Vol. 43, Issue 2, 2006, pp. 236-252.